Eur. Phys. J. B **3**, 169–174 (1998)

THE EUROPEAN PHYSICAL JOURNAL B

Structure, composition and magnetocaloric properties in polycrystalline $La_{1-x}A_xMnO_{3+\delta}$ (A = Na, K)

W. Zhong[1,2,a], W. Chen[1,3], W.P. Ding[2], N. Zhang[1], A. Hu[1], Y.W. Du[1], and Q.J. Yan[2]

[1] National Laboratory of Solid State Microstructures, Nanjing University, Nanjing 210093, P.R. China
[2] Department of Chemistry, Nanjing University, Nanjing 210093, P.R. China
[3] Department of Physics, Hebei Normal University, Shijiazhuang 050091, P. R. China

Received: 12 September 1997 / Revised: 18 December 1997 / Accepted: 21 January 1998

Abstract. The polycrystalline perovskitelike manganese oxides $La_{1-x}A_xMnO_{3+\delta}$ (A = Na, and K, $0.05 < x \leq 0.20$) have been fabricated by sol-gel technique. For all the compositions explored in this work, the average manganese oxidation state is practically constant, at 3.32 ± 0.02 for A = Na, and 3.40 ± 0.04 for A = K, respectively. A close relationship is confirmed to hold between the Curie temperature (T_c) and the bond distance of Mn-O. Results of magnetic measurements show that these materials can be utilized as suitable candidates for magnetic refrigerants with wide applied temperature span, for their significant entropy change and the easily tuned Curie temperature.

PACS. 75.30.Sg Magnetocaloric effect – 82.80.-d Chemical analysis and related physical methods of analysis – 81.05.Mh Cermets, ceramic and refractory composites

1 Introduction

A magnetic-field-induced magnetic entropy change is a well-known technique for magnetic refrigeration. Up to nowadays, the magnetocaloric effects have been extensively studied in two kinds of working substances for magnetic refrigeration: paramagnetic salts and ferromagnetic substances. The former have been conventionally used to obtain low temperature, *e.g.* $T < 15$ K. The most important example is the adiabatic demagnetization of a paramagnetic salt at low temperature, a means by which temperatures as low as 10^{-3} K are attainable. The latter are useful for magnetic refrigeration at high temperature $T > 20$ K; in this temperature range, the Ericsson-cycle has been utilized to remove the effect of lattice entropy [1–3].

Refrigeration in the room temperature range is of particular interest for potential impact on energy savings and environmental concerns. In order to expand effective working temperature (especially near room temperature), a great effort has been made theoretically and experimentally to design a new refrigerator and to search for effective magnetorefrigerants, which have large magnetic entropy change ($-\Delta S_M-$) under a magnetic field [1–7]. According to the Curie-Weiss law for the ferromagnetic, large $-\Delta S_M-$ is expected at Curie temperature T_c with large effective Bohr magneton number $P = g[J(J+1)]^{1/2}$, where g is the g factor and J is the total angular momentum quantum number [2]. In view of above, the previous studies [8,9] mainly concentrated on intermetallic compounds and alloys of rare earths with high J. The largest reported value of $-\Delta S_M-$ in the group of rare earths and their alloy was 13.7 J/kg K for pure gadolinium, which undergoes a ferromagnetic phase transition at 293 K under a magnetic field of $H = 8$ T, therefore Gd is thought to be the optimum magnetic refrigerants used near room temperature [2]. It is of interest to seek other systems which exhibit magnetic phase transitions in the neighborhood of room temperature. One such system is perovskitelike manganese oxides [10–13].

Extensive systematic investigations have been carried out on lanthanide manganites $Ln_{1-x}A_xMnO_3$ (Ln = La, Pr, Nd, Sm; A = Ca, Sr, or Ba) especially in the past three years after the discovery of colossal magnetoresistance in these compounds [14–22]. In fact, the magnetic and electric properties of these materials have been known for a long time. The pure compounds $LnMnO_3$ are antiferromagnetic insulators. Upon doping A^{2+} ions, both Mn^{3+} ($t_{2g}^3e_g^1$) and Mn^{4+} (t_{2g}^3) are present. The e_g electrons are delocalized due to the strong hybrid with the oxygen $2p$ states, and mediate the ferromagnetic interaction between localized t_{2g} spins. Arising from the competition between antiferromagnetic superexchange and ferromagnetic double-exchange interaction, various magnetic structures have been observed with the substitution of Ln and A. Some of perovskite manganese oxides exhibit discontinuous variation in the volume at the ferromagnetic transition, and the associated sharp change in magnetization

[a] e-mail: ufp@netra.nju.edu.cn

[23,24]. The simultaneous structural and magnetic transitions at T_c can strongly influence on the magnetic entropy change. Our research group has measured the magnetic entropy change of perovskitelike manganese oxides, and observed the larger magnetic entropy change in compounds $La_{1-x}Ca_xMnO_3$ ($x = 0.2$, $T_c = 230$ K; $x = 0.33$, $T_c = 257$ K) than that of pure gadolinium upon an field of 1.5 T [11,12].

A good candidate for magnetic refrigerant must possess large magnetic entropy change and suitable T_c. Two different parameters have been considered to be relevant concerning the Curie temperature of these manganites, namely, the concentration of Mn^{4+} (by tuning the composition parameter x or δ, the materials could exhibit very different Curie temperatures, *e.g.*, from 100 to 370 K [17,19]) and the average size of A-site cations, $\langle r_A \rangle$. (The replacement of La by smaller rare-earth ions such as Pr or Y causes a large distortion of the Mn-O-Mn bond, thus decreasing T_c.) Systematic studies have been made on alkaline-earth-doped lanthanide manganites, however, references to magnetic and electronic properties of monovalent alkali-metal-doped materials are very scarce. By taken into consideration that the donor property of alkali-metal is stronger than that of alkaline-earth-metal, it would be expected that alkali-metal-doped manganites exhibit distinguishing feature in structure, electronic behaviour, and magnetic properties from alkaline-earth-doped lanthanide manganites. In the present work, alkali-metal-doped polycrystalline lanthanide manganites $La_{1-x}A_xMnO_{3+\delta}$ (A = Na, K; $x = 0.075$, 0.10, 0.165, and 0.20) have been fabricated by the sol-gel technique in order to obtain high pure and homogeneous powders. The sol-gel method plays an essential role to avoid alkali-metal loss. On the basis of the success of this synthetic approach, several methods such as X-ray diffractometry (XRD), induced coupled plasma (ICP) spectroscopy, transmission electron microscopy (TEM), temperature programmed reduction (TPR), and magnetism measurement (VSM) have been used to obtain detailed information about the structure, composition and magnetocaloric properties in the $La_{1-x}A_xMnO_{3+\delta}$ (A = Na, K) system.

2 Experimental details

Polycrystalline samples of $La_{1-x}A_xMnO_{3+\delta}$(A = Na, K) were synthesized as follows. Stoichiometric amounts of La_2O_3, Na_2CO_3 (or K_2CO_3),and $Mn(NO_3)_2$ were dissolved in dilute HNO_3 solution at 333 K, suitable amounts of citric acid and ethylene glycol as coordinate agent were added and a complete homogeneous transparent solution was achieved. This solution was slowly evaporated at 333 K until a high viscous residual was formed, and a gel was developed during heating at 443 K. The gel was thermally treated at 873 K for 5 hours for the purpose of the organic precursor decomposition. After grinding, the samples were calcined in air at 1273 K for 5 hours and furnace cooled.

The phase identification and structural analysis were performed on an X-ray powder diffractometer (Model D/Max-RA, Rigaku, Japan). High-purity silicon powder was used as an internal standard for the lattice parameter determination. The metal content in the sintered sample was determined by the induced coupled plasma (ICP) spectroscopy (Model 1100 + 2000, Jarrell-Ash, USA). The morphology of $La_{1-x}A_xMnO_{3+\delta}$ was examined by direct observation *via* transmission electron microscopy (TEM) (Model JEM-200 CX, JEOL, Japan).

The oxygen content in these materials was determined by a temperature-programmed reduction (TPR) technique [25,26]. TPR is a useful method, which is highly sensitive and does not depend on any specific property of the sample other than the species under study be in a reducible condition. Generally, the reaction between metal oxide MO and hydrogen to form metal M and water vapor can be represented by the general equation

$$MO(s) + H_2 \rightarrow M(s) + H_2O(g). \quad (1)$$

If the standard free energy change for the reaction ΔG° is negative, the reductions for these oxides are thermodynamically feasible. However, since

$$\Delta G = \Delta G^\circ + RT \log(P_{H_2O}/P_{H_2}) \quad (2)$$

it may still be possible for the reduction to proceed even when ΔG° is positive. The TPR experimental method is such that the water vapor is constantly swept from the reaction zone as it is formed. Thus if P_{H_2O} is lowered sufficiently at elevated temperatures, it is possible that the term RT log (P_{H_2O}/P_{H_2}) could be sufficiently negative to nullify a positive ΔG°.

In our present experiment, Ar + H_2 (18.5% V/V) mixed gas flushed over the sample, which was heated at a linear rate (6 K/min), and the concentration of H_2 in mixed gas was monitored simultaneously by thermal conductivity detector (TCD). The oxygen content in sample was deduced from the consumption of H_2 in reaction between H_2 and the sample, based on following equation (In fact, the valences of lanthanum and alkali-metal were conserved, while the Mn^{3+}, Mn^{4+} were reduced to Mn^{2+} in the reaction):

$$La_{1-x}A_xMnO_{3+\delta} + H_2 \rightarrow La_2O_3 + AOH + MnO + H_2O. \quad (3)$$

The dependence of magnetization on temperature was measured using a vibrating sample magnetometer (VSM). The Curie temperature T_c defined as the temperature of the maximum slope in dM/dT, was extracted from the low field magnetization (0.5 T) *versus* temperature rather than from saturation versus temperature, because the high field magnetization could shift the Curie temperature several degrees [7].

3 Results and discussion

3.1 Structure and composition

The crystallite size of these samples observed directly by TEM is 250−300 nm (A = K), and 350−500 nm

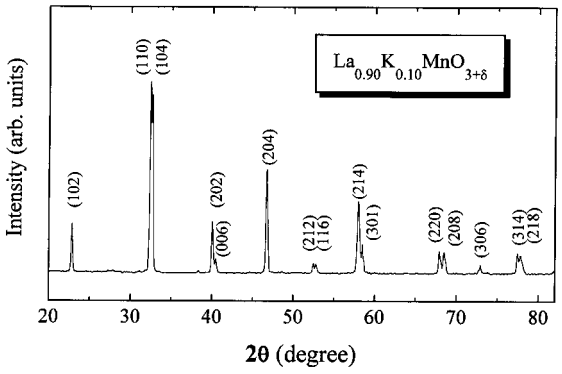

Fig. 1. X-ray diffraction pattern of $La_{0.90}K_{0.10}MnO_{3+\delta}$ sample.

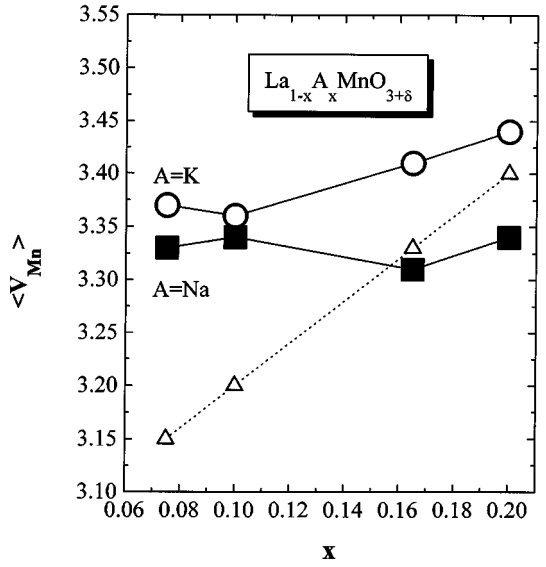

Fig. 2. Average manganese valence ($\langle V_{Mn}\rangle$) *versus* dope level (x) for $La_{1-x}A_xMnO_{3+\delta}$. Open circles are the data for A = K, solid squares are for A = Na, and open up triangles are for the theoretical values of average Mn valence for $La_{1-x}A_xMnO_3$.

(A = Na), respectively. The X-ray diffraction pattern of $La_{0.90}K_{0.10}MnO_{3+\delta}$ is shown in Figure 1. For all the studied compositions, $0.05 < x \leq 0.20$, $La_{1-x}A_xMnO_{3+\delta}$ (A = Na, K) materials have the rhombohedral perovskite structure without any other secondary or impurity phase.

Table 1 summarizes the results of the ICP and TPR measurements. As can be seen, the actual alkali-metal content for all the compositions explored in this work is practically equal to the nominal one. Tofield and Scott [27], and Roosmalen [28] reported that cation vacancies exist both in A and B sites instead of oxygen interstitials by the neutron technique, therefore, the composition of $La_{1-x}A_xMnO_{3+\delta}$ is better expressed as $La_{(3-3x)/(3+\delta)}A_{3x/(3+\delta)}Mn_{3/(3+\delta)}O_{3.00}$ [29]. The average manganese oxidation state calculated from electric neutrality is also listed in Table 1. Figure 2 shows the plot of the average manganese oxidation state $\langle V_{Mn}\rangle$ *versus* dope level x, the theoretical expected values of $\langle V_{Mn}\rangle$ for

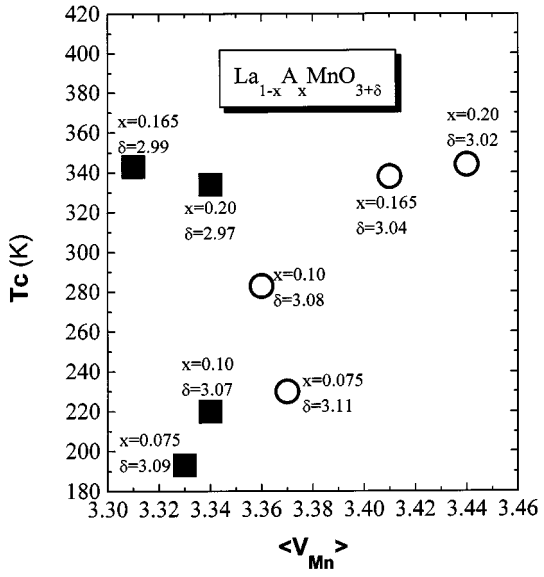

Fig. 3. Plot of Curie temperature (T_c) *versus* average manganese valence ($\langle V_{Mn}\rangle$) in polycrystalline $La_{1-x}A_xMnO_{3+\delta}$. Open circles are the data for A = K, solid squares are for A = Na.

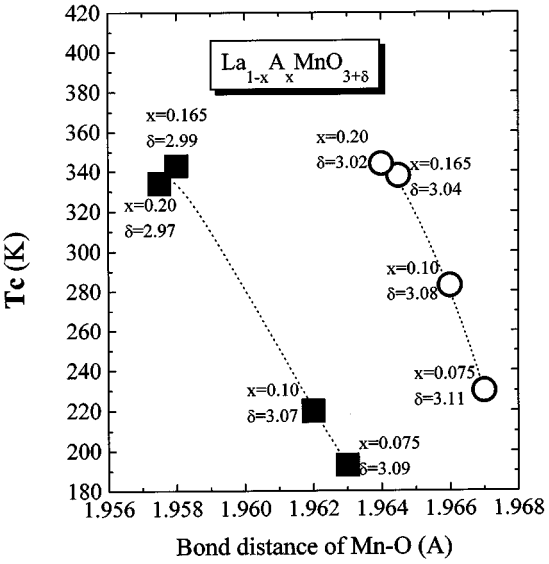

Fig. 4. Plot of Curie temperature (T_c) as a function of Mn-O distance in $La_{1-x}A_xMnO_{3+\delta}$. Solid squares are the data for A = Na, open circles are for A = K. Lines through the points are guides to the eye.

$La_{1-x}A_xMnO_3$ are also shown in Figure 2. One can observe that there is no clear correlation between the x and the $\langle V_{Mn}\rangle$, in contrast with the expected monotonic linear increase with x. In fact, for all the compositions, the average manganese oxidation state $\langle V_{Mn}\rangle$ is practically constant, at 3.32 ± 0.02 for A = Na, and 3.40 ± 0.04 for A = K, respectively. The increase in the alkali-metal content makes a decrease in oxygen excess. Similar phenomena have been reported for the $La_{1-x}K_xMnO_{3+\delta}$ system by Ng-Lee *et al.* [30]

Table 1. Summary of the results of ICP and TPR measurements.

x^+	La/Mn	A/Mn	$\langle V_{Mn}\rangle^*$	δ	stoichiometry
			A = Na		
0.075	0.925	0.074	3.33	0.09	$La_{0.898}Na_{0.072}Mn_{0.971}O_{3.00}$
0.100	0.901	0.101	3.34	0.07	$La_{0.880}Na_{0.099}Mn_{0.977}O_{3.00}$
0.165	0.834	0.163	3.31	− 0.01	$La_{0.834}Na_{0.163}Mn_{1.000}O_{2.99}$
0.200	0.799	0.199	3.34	− 0.03	$La_{0.799}Na_{0.199}Mn_{1.000}O_{2.97}$
			A = K		
0.075	0.926	0.073	3.37	0.11	$La_{0.893}K_{0.070}Mn_{0.965}O_{3.00}$
0.100	0.900	0.099	3.36	0.88	$La_{0.877}K_{0.096}Mn_{0.974}O_{3.00}$
0.165	0.835	0.164	3.41	0.04	$La_{0.813}K_{0.160}Mn_{0.987}O_{3.00}$
0.200	0.801	0.197	3.44	0.02	$La_{0.796}K_{0.196}Mn_{0.993}O_{3.00}$

$^+$ calculated value, * the average manganese oxidation state

Table 2. Summary of the magnetic entropy change at T_c and the heat originated only from magnetic entropy change between $T_c \pm 25$ K for samples $La_{1-x}A_xMnO_{3+\delta}$ upon an applied field $H_{max} = 1.0$ T.

Sample	Curie temperature T_c (K)	Entropy change $\lvert\Delta S_M(T_c, 1.0\text{ T})\rvert$ (J/kg K)	Heat $\lvert\Delta Q_{MS}(T_c \pm 25\text{ K},\ 1.0\text{ T})\rvert$ (J/kg)
Pure Gd	293	3.27	92.0
$La_{0.898}Na_{0.072}Mn_{0.971}O_{3.00}$	193	1.32	56.1
$La_{0.880}Na_{0.099}Mn_{0.977}O_{3.00}$	220	1.53	59.4
$La_{0.834}Na_{0.163}Mn_{1.000}O_{2.99}$	343	2.11	60.4
$La_{0.799}Na_{0.199}Mn_{1.000}O_{2.97}$	334	1.96	73.7
$La_{0.893}K_{0.070}Mn_{0.965}O_{3.00}$	230	0.78	37.6
$La_{0.877}K_{0.096}Mn_{0.974}O_{3.00}$	283	1.10	48.6
$La_{0.813}K_{0.160}Mn_{0.987}O_{3.00}$	338	1.53	56.1
$La_{0.796}K_{0.196}Mn_{0.993}O_{3.00}$	344	1.55	55.5

Figure 3 displays the plot of T_c *versus* $\langle V_{Mn}\rangle$. Surprisingly, one could not find a close relationship between the the average manganese oxidation state and T_c, although this relationship could be observed in alkaline-earth-doped lanthanide manganites. Figure 4 shows the variation of T_c with the bond distance of Mn–O determined by the XRD analysis. One can see that T_c tends to increase when the Mn–O distance decreases. In frame of the double-exchange interaction theory, shorter Mn–O distance in this structure, corresponds to the larger Mn–O–Mn bonding angle, leads to a stronger interaction, and the higher T_c.

3.2 Magnetocaloric properties

It has been suggested that the classical magnetization measurements be a powerful tool to select the suitable magnetorefrigerants [3]. From the thermodynamic theory, the magnetic entropy change $\Delta S_M(T, H)$ is given by [2]

$$\Delta S_M(T,H) = S_M(T,H) - S_M(T,0) = \int_0^H (\frac{\partial M}{\partial T})dH. \quad (4)$$

For magnetization measured at discrete field and temperature intervals, the magnetic entropy change ΔS_M can be approximated by [7]

$$|\Delta S_M| = \sum \frac{1}{T_{i+1} - T_i}(M_i - M_{i+1})_H \Delta H_i \quad (5)$$

where M_i and M_{i+1} are the magnetization values measured in a field H at temperature T_i and T_{i+1}, respectively. The change of specific heat associated with the magnetization equals

$$\Delta C_{P,H} = T\frac{\partial(\Delta S_M)}{\partial T}\,. \quad (6)$$

Thus, if the contribution of electrons and lattice to the specific heat is known, the temperature dependence of can be obtained.

Isothermal magnetization curves were measured in a field up to 1.0 T. Magnetization measurements were repeated for 10, 5, or 3 K temperature steps. The temperature steps were smaller near transition temperature, and larger further away. By using the equation (4), $\Delta S_M(T, H)$ is obtained, and Figure 5 shows the magnetic entropy

Table 3. Magnetic entropy change $|\Delta S_M|$ near room temperature (> 250 K) for some alkaline-earth-doped lanthanide manganites.

Sample[+]	Curie temperature T_c (K)	Magnetic field H_{max} (T)	Entropy change $\lvert\Delta S_M(T_c)\rvert$ (J/kg K)	Ref.
$La_{0.67}Ca_{0.33}MnO_3$(f)	250	1.0	0.5	10
$La_{0.67}Sr_{0.33}MnO_3$(f)	350	5.0	1.7	10
$La_{0.67}Ba_{0.33}MnO_3$(f)	290	5.0	1.3	10
$La_{0.67}Ca_{0.33}MnO_\delta$(p)	260	1.0	1.1	13
$La_{0.75}Sr_{0.15}Ca_{0.1}MnO_3$(p)	330	1.5	2.7	12
$La_{0.75}Sr_{0.125}Ca_{0.125}MnO_3$(p)	280	1.5	1.5	12

[+] "*f*" denotes film; "*p*" denotes polycrystalline sample

changes as a function of temperature for $La_{1-x}A_xMnO_{3+\delta}$ samples at applied field $H_{max} = 1.0$ T. The peak temperature of $|\Delta S_M|$ is the same as T_c.

In order to make a comparison of the magnetocaloric properties between $La_{1-x}A_xMnO_{3+\delta}$ and pure Gd, we also measured the magnetic entropy change of Gd, and obtained $|\Delta S_M| \sim 3.27$ J/kg K at T_c (293 K) for $H_{max} = 1.0$ T; the value agrees with reference [7]. The maximum $|\Delta S_M|$ of $La_{1-x}A_xMnO_{3+\delta}$ is lower than that of pure Gd, but the broader $|\Delta S_M|$ distribution for $La_{1-x}A_xMnO_{3+\delta}$ is obtained.

The heat originated only from magnetic entropy change between $T_c \pm 25$ K can be calculated by

$$|Q_{MS}(T_c \pm 25 \text{ K},\ 1.0 \text{ T})| = \int_{T_c-25}^{T_c+25} |\Delta S_M(T, 1.0T)| dT \tag{7}$$

The data of $|Q_{MS}(T_c \pm 25 \text{ K},\ 1.0\text{T})|$ are listed in Table 2.

In the neighborhood of room temperature (> 250 K), $La_{1-x}A_xMnO_{3+\delta}$ system has significant $|\Delta S_M|$ compared with alkaline-earth-doped lanthanide manganites (see Tab. 3). These results reveal that alkali-metal-doped lanthanide manganites are more suitable candidates for magnetic refrigerants with wider applied temperature span, for their significant entropy change and easily tuned Curie temperature. Compared with rare earth metals and their alloys, the $La_{1-x}A_xMnO_{3+\delta}$ samples have advantages as follows: (i) easily tuned Curie temperature by changing the material composition x and d, (ii) a constant magnetic entropy change against temperature variation would be obtained by mixing several kinds of samples with different T_c, (iii) a quite large magnetic entropy change upon a low magnetic field, (iv) distribution is broader, (v) higher chemical stability and lower cost, and (vi) considerable small magnetic hysteresis and isotropic.

This work is supported by the National Climbing Program, P.R. China.

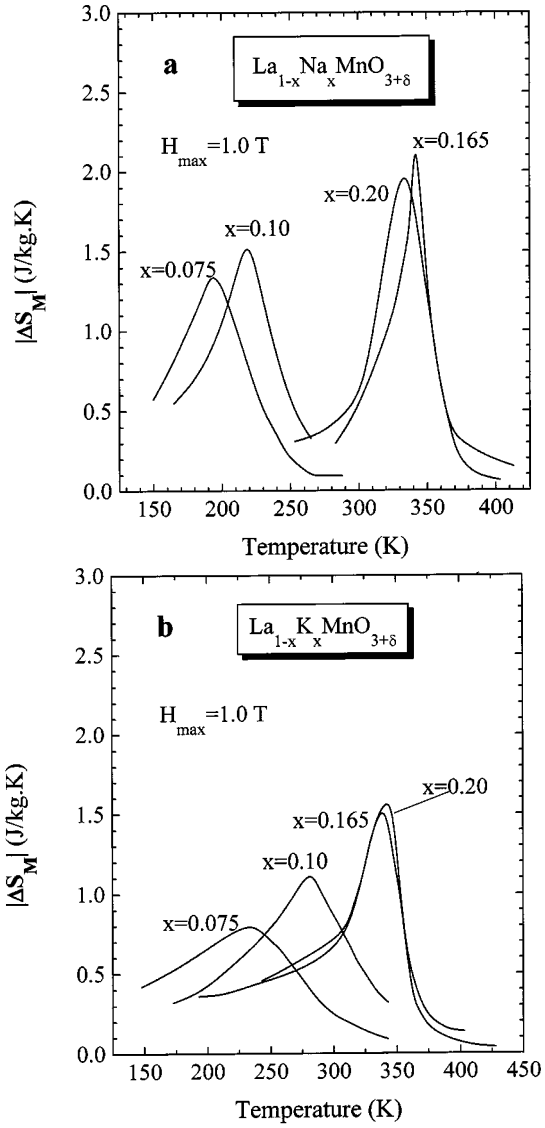

Fig. 5. Temperature dependence of magnetic entropy change upon an external field $H_{max} = 1.0$ T for (a) $La_{1-x}Na_xMnO_{3+\delta}$ and (b) $La_{1-x}K_xMnO_{3+\delta}$.

References

1. G.V. Brown, J. Appl. Phys. **47**, 3673 (1976).
2. T. Hashimoto, T. Numasawa, M. Shino, T. Okada, Cryogenics **21**, 647 (1981).
3. R.D. McMichael, J.J. Ritter, R.D. Shull, J. Appl. Phys. **73**, 6946 (1993).
4. H. Oesterreicher, F.T. Parker, J. Appl. Phys. **55**, 4334 (1984).
5. K.A. Gschneidner, H. Takeya Jr., J.O. Moorman, V.K. Pecharsky, Appl. Phys. Lett. **64**, 253 (1994)
6. H. Takeya, V.K. Pecharsky, K.A. Gschneidner Jr., J.O. Moorman, Appl. Phys. Lett. **64**, 2739 (1994)
7. M. Foldeaki, R. Chahine, T.K. Bose, J. Appl. Phys. **77**, 3528 (1995).
8. K. Adachi, J. Phys. Soc. Jpn **61**, 2187 (1961).
9. T. Hashimoto, T. Kuzuhara, M. Sahashi, K. Inomata, A. Tomokiyo, H. Yayama, J. Appl. Phys. **62**, 4873 (1987)
10. D.T. Morelli, A.M. Mance, J.V. Mantese, A.L. Micheli, J. Appl. Phys. **79**, 373 (1996)
11. Z.B. Guo, J.R. Zhang, H. Huang, W.P. Ding, Y.W. Du, Appl. Phys. Lett. **70**, 904 (1997)
12. Z.B. Guo, Y.W. Du, J.S. Zhu, H. Huang, W.P. Ding, D. Feng, Phys. Rev. Lett. **78**, 1142 (1997)
13. X.X. Zhang, J. Tejada, Y. Xin, G.F. Sun, K.W. Wong, X. Bohigas, Appl. Phys. Lett. **69**, 3596 (1996).
14. R. Von Helmolt, J. Wecker, B. Holzapfel, L. Schultz, K. Samwer, Phys. Rev. Lett. **71**, 2331 (1993).
15. G.Q. Gong, C. Canedy, G. Xiao, J.Z. Sun, A. Gupta, W.J. Gallagher, Appl. Phys. Lett. **67**, 1783 (1995).
16. S. Jin, T.H. Tiefel, M. McCormack, R.A. Fastnacht, R. Ramesh, L.H. Chen, Science **264**, 413 (1994).
17. J.M.D. Coey, M. Viret, L. Ranno, K. Ounadjela, Phys. Rev. Lett. **75**, 3910 (1995).
18. Y. Moritomo, A. Asamitsu, Y. Tokura, Phys. Rev. B, **51**, 16491 (1995).
19. R. Mahendiran *et al.*, Phys. Rev. B **53**, 3348 (1996).
20. H.L. Liu, C. Kwon, Q. Li, R.L. Greene, T. Venkatesan, Appl. Phys. Lett. **65**, 2108 (1994).
21. P. Schiffer, Z.A.P. Ramirez, W. Bao, S.W. Cheong, Phys. Rev. Lett. **75**, 3336 (1995).
22. J. Barratt, M.R. Lees, G. Balakrishnan, D. McK. Paul, Appl. Phys. Lett. **68**, 424 (1996).
23. P.G. Radaelli *et al.*, Phys. Rev. Lett. **75**, 4488 (1995).
24. M.R. Ibarra *et al.*, Phys. Rev. Lett. **75**, 3541 (1995).
25. N.W. Hurst *et al.*, Catal. Rev. **24**, 233 (1982).
26. T. Nakamura, G. Petzow, L.J. Gauckler, Mat. Res. Bull. **14**, 649 (1979).
27. B.C. Tofield, W.R. Scott, J. Solid State Chem. **10**, 183 (1974).
28. J.A.M. Van Roosmalen *et al.*, J. Solid State Chem. **91**, 225 (1991).
29. J. Topfer, J.B. Goodenough, Chem. Mater. **9**, 1467 (1997).
30. J. Ng-Lee *et al.*, J. Mater. Chem. **7**, 1905 (1997).